

Supporting Information for

Radar attenuation demonstrates advective cooling in the Siple Coast ice streams

Benjamin H. Hills^{1,2}, Knut Christianson¹, Robert Jacobel³, Howard Conway¹, Rickard Pettersson⁴

¹*Department of Earth and Space Sciences, University of Washington, Seattle, WA, USA*

²*Polar Science Center, Applied Physics Laboratory, University of Washington, Seattle, WA, USA*

³*Department of Physics, St Olaf College, Northfield, MN, USA*

⁴*Department of Earth Sciences, Uppsala University, Uppsala, Sweden*

Table of Contents

S1. SUPPLEMENTAL RADAR LINES	2
<i>FIGURE S1.....</i>	2
<i>FIGURE S2.....</i>	2
<i>FIGURE S3.....</i>	3
S2. ROBIN SOLUTION	4
<i>FIGURE S4.....</i>	4
S3. MEYER SOLUTION	5
<i>FIGURE S5.....</i>	5
<i>TABLE S1.....</i>	6

S1. Supplemental Radar Lines

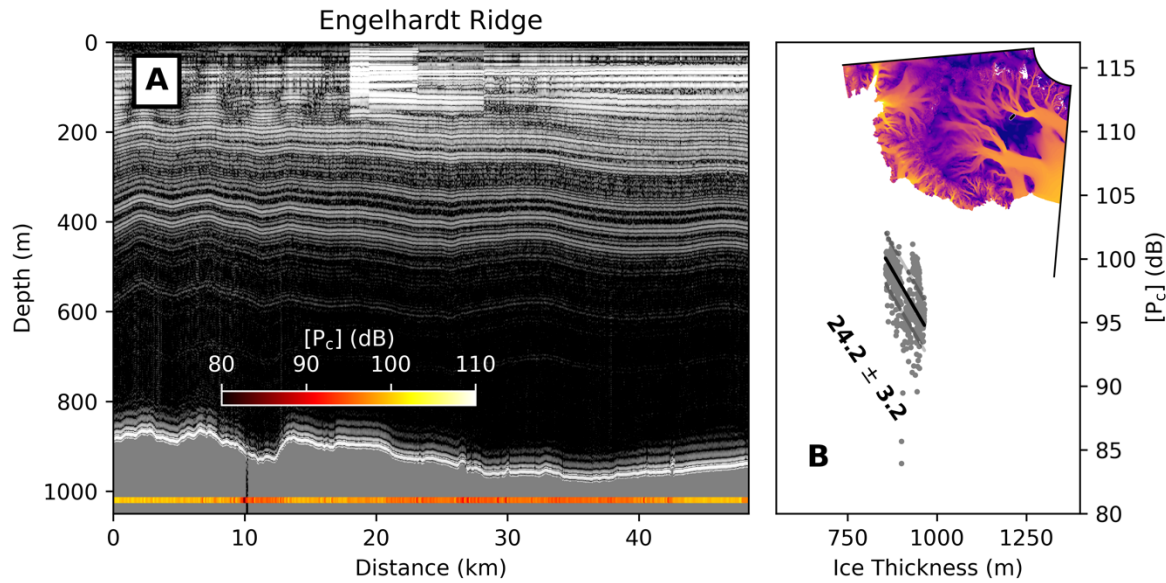


Figure S1. As in Figure 2 but for Engelhardt Ridge (Nereson and Raymond, 2007). These data are publicly archived at <https://doi.org/10.7265/N52B8VZP>. With minimal thickness variation, this attenuation rate is poorly constrained.

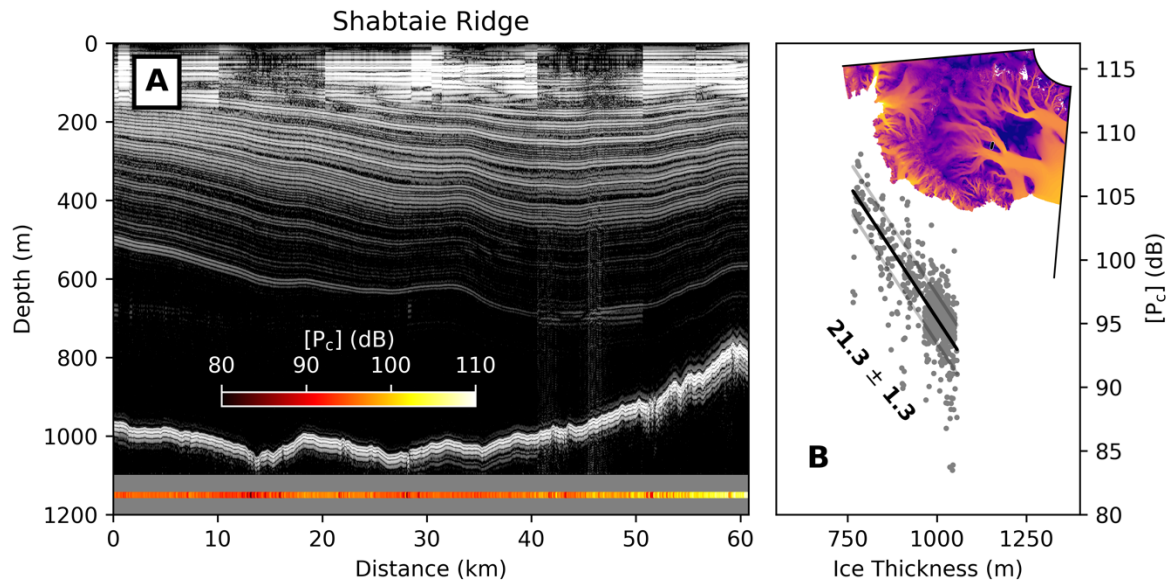


Figure S2. As in Figure 2 but for Shabtaie Ridge (Nereson and Raymond, 2007). These data are publicly archived at <https://doi.org/10.7265/N52B8VZP>.

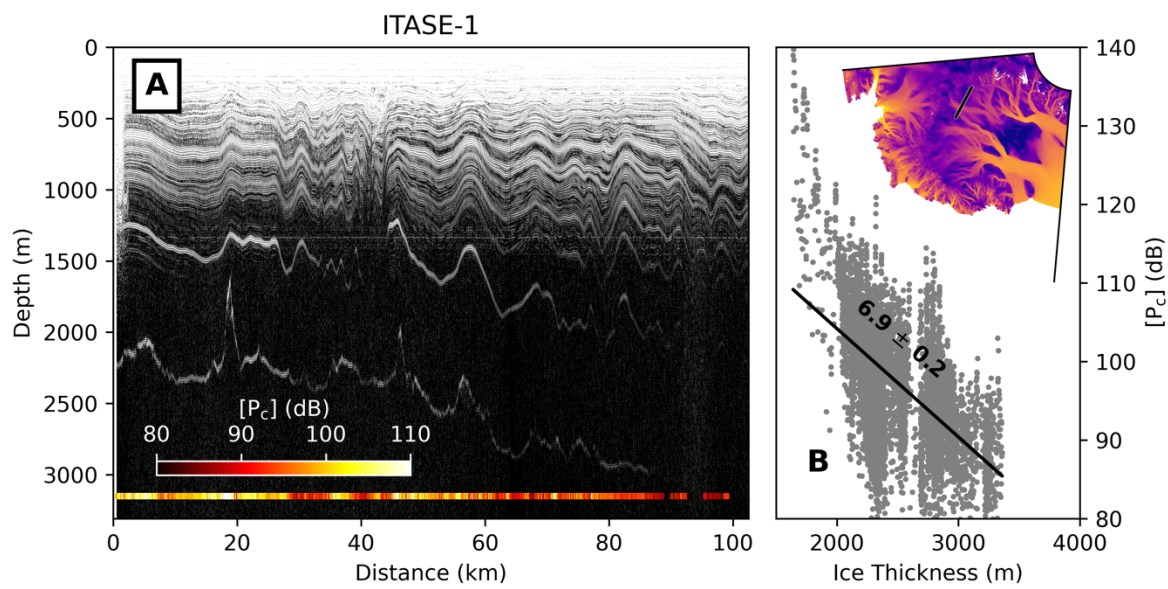


Figure S3. As in Figure 2 but for the ITASE-1 traverse (Jacobel et al., 2005; Welch & Jacobel, 2005).

S2. Robin Solution

Following Cuffey and Paterson (2010) chapter 9.5, the Robin (1955) analytical solution for ice temperature is

$$T = T_s + z_* \frac{\sqrt{\pi}}{2} \left[\frac{dT}{dz} \right]_{bed} \left(\operatorname{erf}\left(\frac{z}{z_*}\right) - \operatorname{erf}\left(\frac{H}{z_*}\right) \right) \quad (\text{S1})$$

where the characteristic thickness is

$$z_* = \sqrt{\frac{2\alpha H}{\dot{a}}} \quad (\text{S2})$$

and the error function is

$$\operatorname{erf}(z) = \frac{2}{\sqrt{\pi}} \int_0^z \exp(-y^2) dy \quad (\text{S3})$$

In Figure S4, we compare this analytical solution to our numerical solution under the same conditions. Then we compare to the numerical solution with a nonlinear vertical velocity profile (Lliboutry (1979) shape factor; p=5).

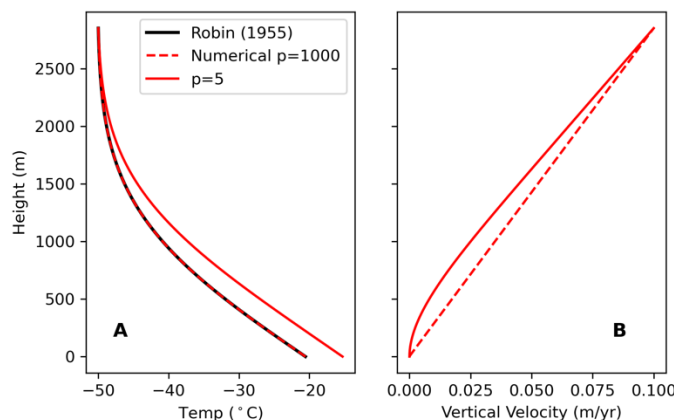


Figure S4. Reproduction of the Robin (1955) analytical solution for ice temperature with parameters from Siple Dome.

S3. Meyer Solution

Following Meyer and Minchew (2018) equation (13), the analytical solution for ice temperature in an ice-stream shear margin is,

$$T = \begin{cases} T_s + \Delta T \frac{Br - \Lambda}{Pe} \left[1 - \frac{z}{H} + \frac{1}{Pe} \exp \left\{ Pe \left(\frac{\xi}{H} - 1 \right) \right\} - \frac{1}{Pe} \exp \left\{ Pe \left(\frac{\xi - z}{H} \right) \right\} \right]; \xi \leq z \leq H \\ T_m; 0 \leq z \leq \xi \end{cases} \quad (S4)$$

with the same variables (Table S1) as in the main manuscript, and all ice properties constant so that it can be solved analytically.

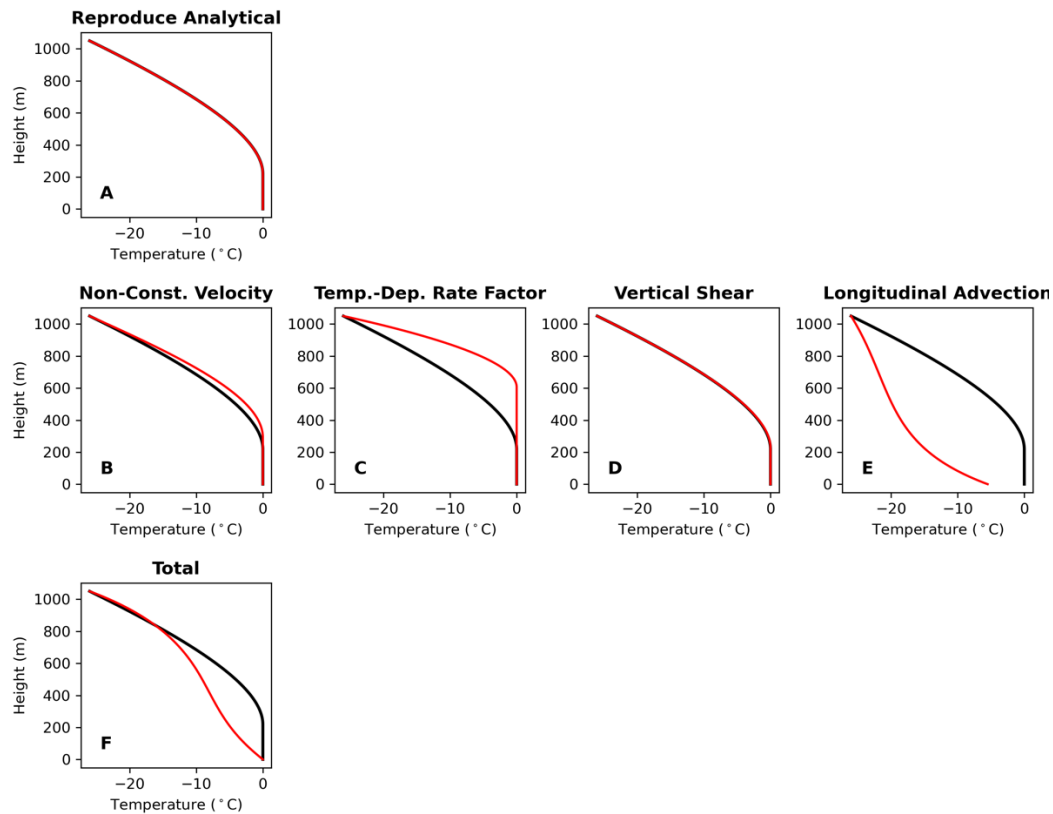


Figure S5. Reproduction of the Meyer and Minchew (2018) analytical solution (black) for ice temperature with parameters from the Dragon Shear Margin. (A) Direct reproduction of the analytical solution with the numerical model (red). (B-E) Isolated temperature effect of each physical process. (F) Effective temperature solution at the Dragon Shear Margin in the case of a stiff ice column as in Figure 7B.

Table S1. Model variables.

Variable	Name	Value	Units
Pe	Peclet number	-	-
Br	Brinkman number	-	-
Λ	Dimensionless Longitudinal Advection	-	-
t	Time	-	s
x^*	Longitudinal (along-flow) coordinate	-	m
L	Characteristic length scale	-	m
y^*	Lateral (across-flow) coordinate	-	m
z	Vertical coordinate	-	m
H	Ice Thickness	-	m
z_*	Characteristic ice thickness	-	m
ζ	Temperate ice thickness	-	m
u^*	Longitudinal velocity	-	$m\ s^{-1}$
w	Vertical velocity	-	$m\ s^{-1}$
T	Temperature	-	K
T_s	Surface temperature	-	K
ΔT	Temperature difference (bed – surface)	-	K
\dot{a}	Accumulation rate	-	$m\ s^{-1}$
$\dot{\epsilon}$	Strain rate	-	s^{-1}
τ	Shear stress	-	Pa
Q	Strain heat source	-	W
g	Gravity	9.81	$m\ s^{-2}$
ρ	Density of ice	917	$kg\ m^{-3}$
c	Heat capacity of ice	2097	$J\ kg^{-1}\ K^{-1}$
k	Thermal conductivity of ice	2.1	$W\ m^{-1}\ K^{-1}$
α	Thermal diffusivity of ice	1.09x10 ⁻⁶	$m^2\ s$
θ	Surface slope	-	rad
A	Rate factor	-	$Pa^{-n}\ s^{-1}$
n	Creep exponent	3	-
E	Activation energy (at $T < -10^\circ C$)	6x10 ⁴	$J\ mol^{-1}$
E	Activation energy (at $T > -10^\circ C$)	1.15x10 ⁵	$J\ mol^{-1}$
R	Ideal gas constant	8.32	$J\ K^{-1}\ mol^{-1}$
A_*	Prefactor	-	$Pa^{-n}\ s^{-1}$

References

- Cuffey, K., & Paterson, W. S. B. (2010). *The Physics of Glaciers* (Fourth). Butterworth-Heinemann.
- Jacobel, R. W., Welch, B. C., Steig, E. J., & Schneider, D. P. (2005). Glaciological and climatic significance of Hercules Dome, Antarctica: An optimal site for deep ice core drilling. *Journal of Geophysical Research: Earth Surface*, 110(1), 1–9.
<https://doi.org/10.1029/2004JF000188>
- Lliboutry, L. (1979). A critical review of analytical approximate solutions for steady state velocities and temperatures in cold ice-sheets. *Gletscherkd. Glazialgeol.*, 15(2), 135–148.
- Meyer, C. R., & Minchew, B. M. (2018). Temperate ice in the shear margins of the Antarctic Ice Sheet: Controlling processes and preliminary locations. *Earth and Planetary Science Letters*, 498, 17–26. <https://doi.org/10.1016/j.epsl.2018.06.028>
- Robin, G. de Q. (1955). Ice movement and temperature distribution in glaciers and ice sheets. *Journal of Glaciology*, 2(18), 523–532.
- Welch, B. C., & Jacobel, R. W. (2005). Bedrock topography and wind erosion sites in East Antarctica: Observations from the 2002 US-ITASE traverse. *Annals of Glaciology*, 41, 92–96. <https://doi.org/10.3189/172756405781813258>